Subsurface model inversion

Pushing the limits of subsurface resolution

Musa Maharramov[1] and Biondo L. Biondi[2]*

Stanford Exploration Project

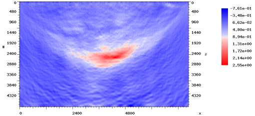

April 17-20, 2017

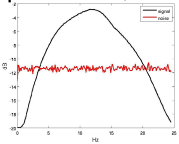

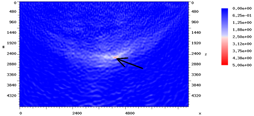

[1]presently ExxonMobil Upstream Research Company; formerly Stanford Exploration Project
[2]Stanford Exploration Project; presenting author

Subtle subsurface change indicators

- Fluid movement ⇒ subsurface velocity changes.
- Stress changes ⇒ subsurface velocity changes.
- **Simultaneous regularized 4D FWI** can resolve significant model changes at a reservoir/overburden scale (Maharramov et al, 2016).
- **Question**: Can FWI **resolve subtle model changes** associated with continuous subsurface stressing?
- **Question**: Can FWI **resolve relative magnitudes of changes** to understand the evolution of subsurface stress?

- Dependence of acoustic velocity V on isotropic effective stress P can be described empirically:

$$V = V_\infty \left(1 - A \exp - \frac{P}{P_0}\right), \quad (1)$$

where V_∞, A, P_0 are positive fitting constants for various types of rocks (Domenico, 1977; Zimmer, 2003; Lee, 2003; Johnston, 2013).

- Note the **flattening of velocity for large effective stress**.

- High-stress anomalies may be localized and "**spiky**", e.g. near the tips of slipping faults.

Response to effective stress change (from Zimmer (2003))

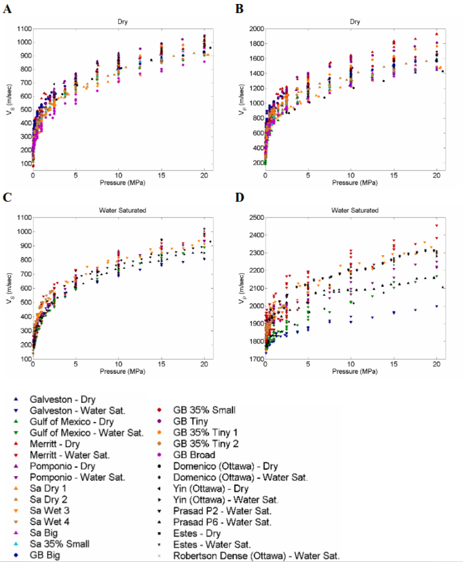

Response of loose quartz layers to shear (from Knuth et al. (2013))

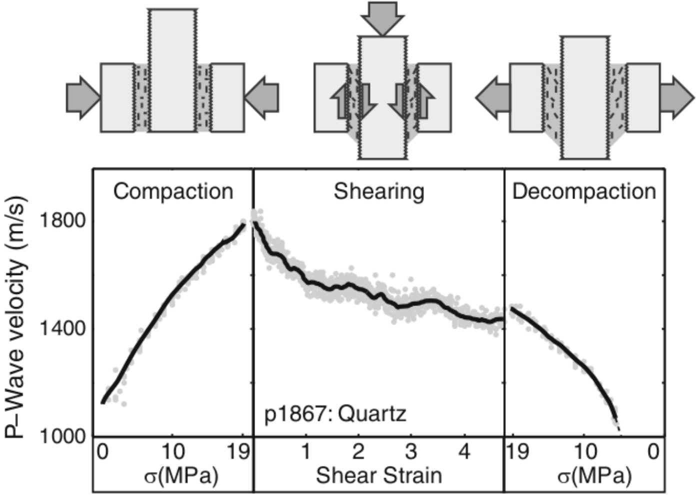

Total-variation difference regularization to extract "**blocky**" changes

- STAGE 1: *Simultaneous FWI* of baseline and monitor with the *total-variation* (TV) difference regularization (Maharramov et al, 2016):

$$\text{Baseline Misfit} + \text{Monitor Misfit} + \tag{2}$$

$$\alpha \| |\nabla \mathbf{W}_m [\mathbf{m}_m - \mathbf{m}_b] | \|_1 . \tag{3}$$

- The total-variation (TV) seminorm (3) promotes model **blockiness** while reducing spurious oscillations.

Field data example: "blocky" Δv due to overburden dilation

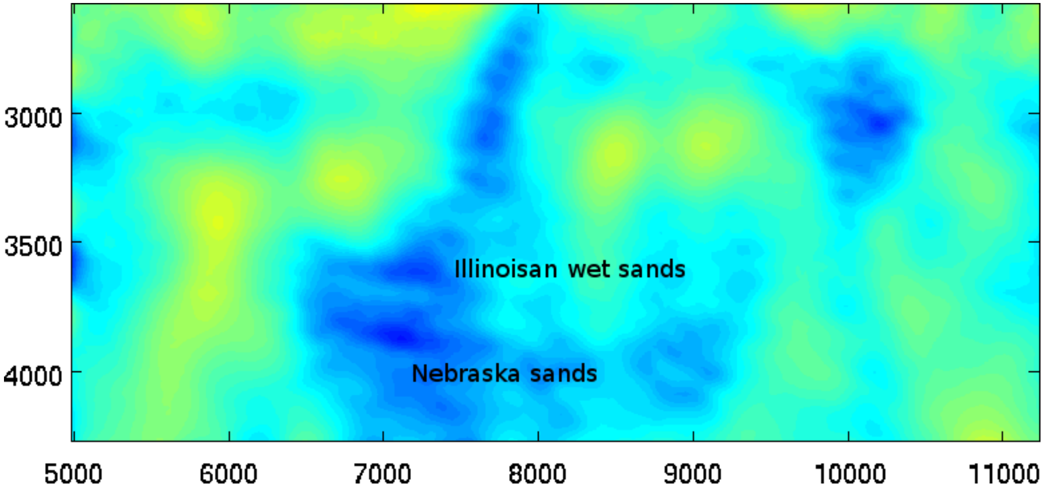

Field data: Δs vs image difference (Maharramov et al, 2016)

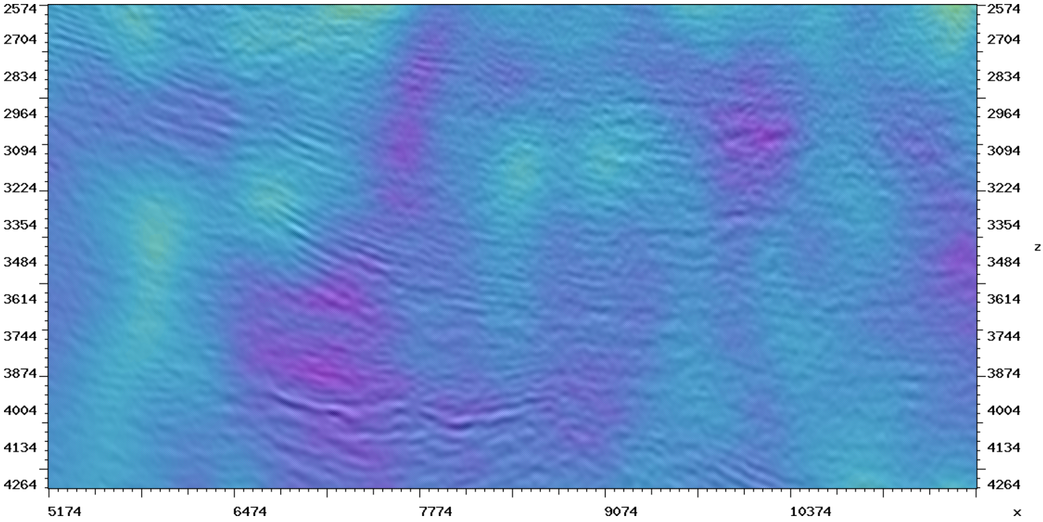

Analysis of depth-shifts in migrated images prestack images

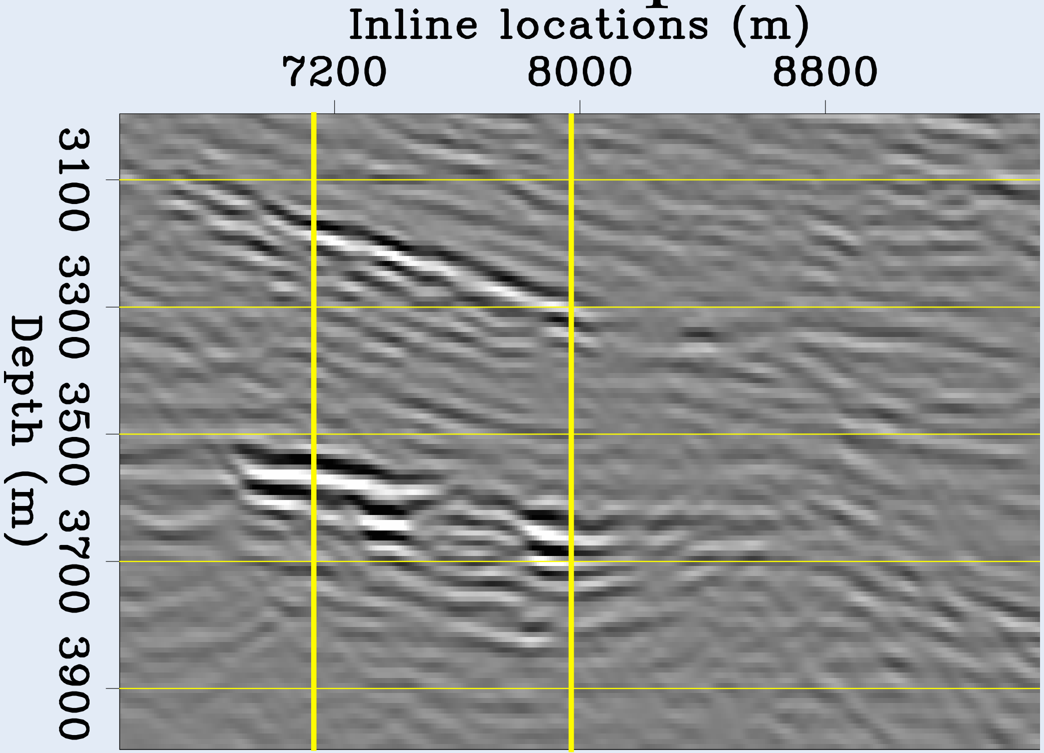

Anisotropic migration of baseline

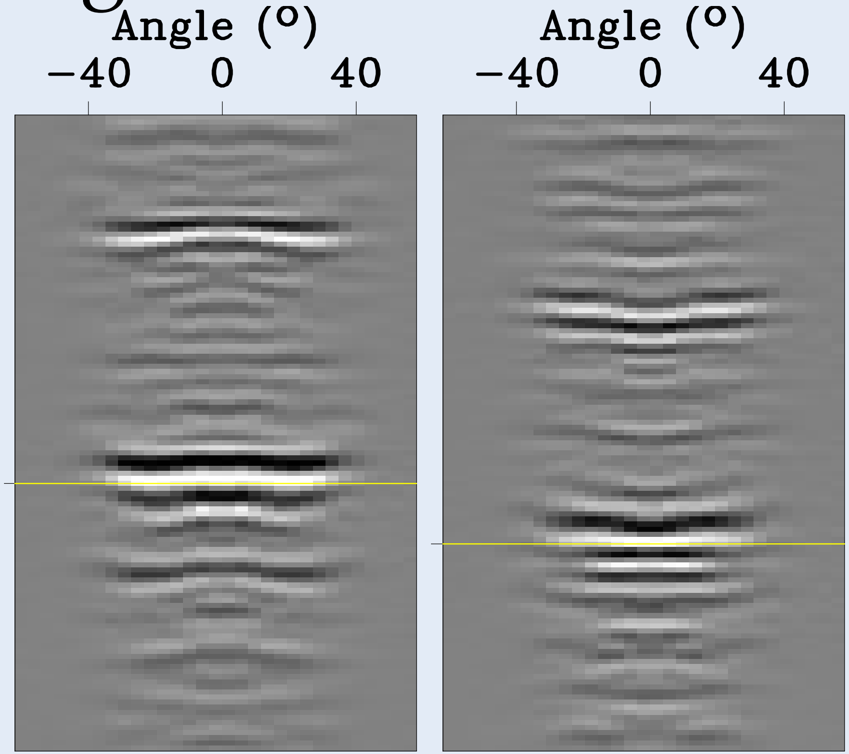

Angle gathers of baseline

Analysis of depth-shifts in migrated images prestack images

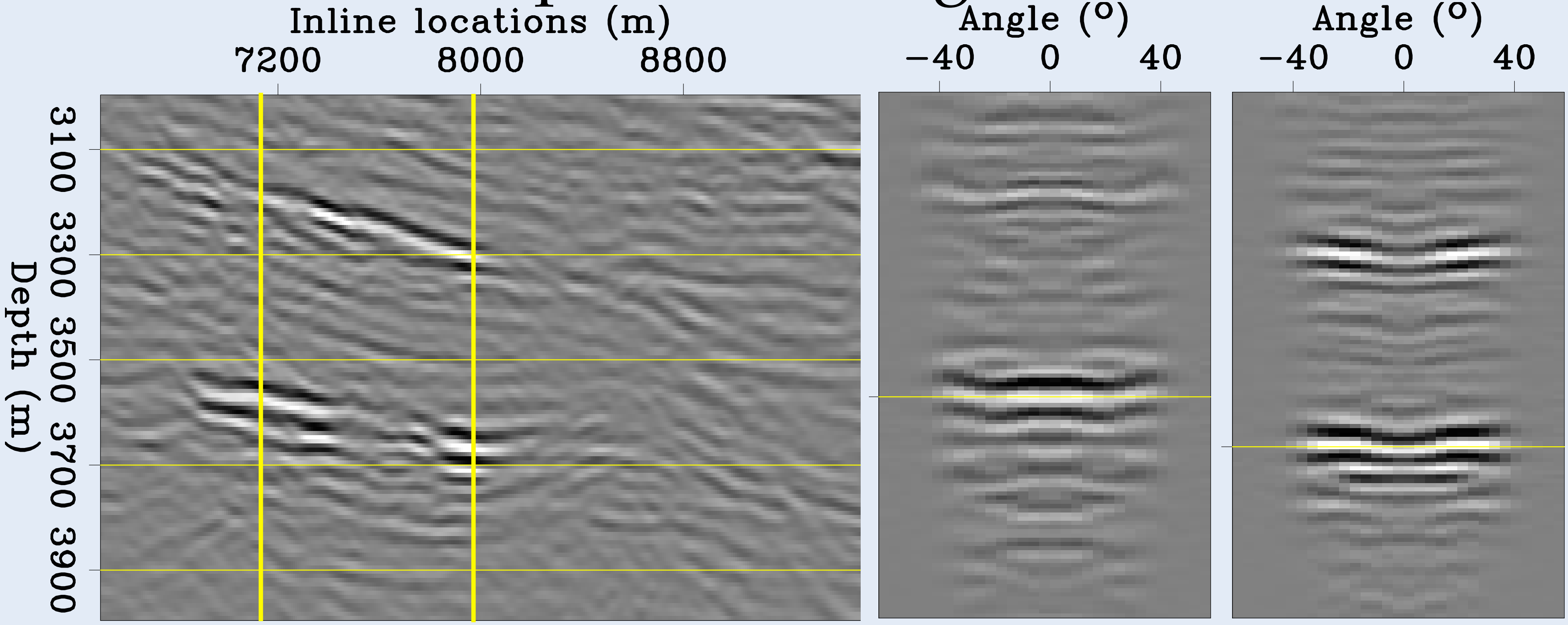

Anisotropic migration of monitor

Angle gathers of monitor

Analysis of depth-shifts in migrated images prestack images

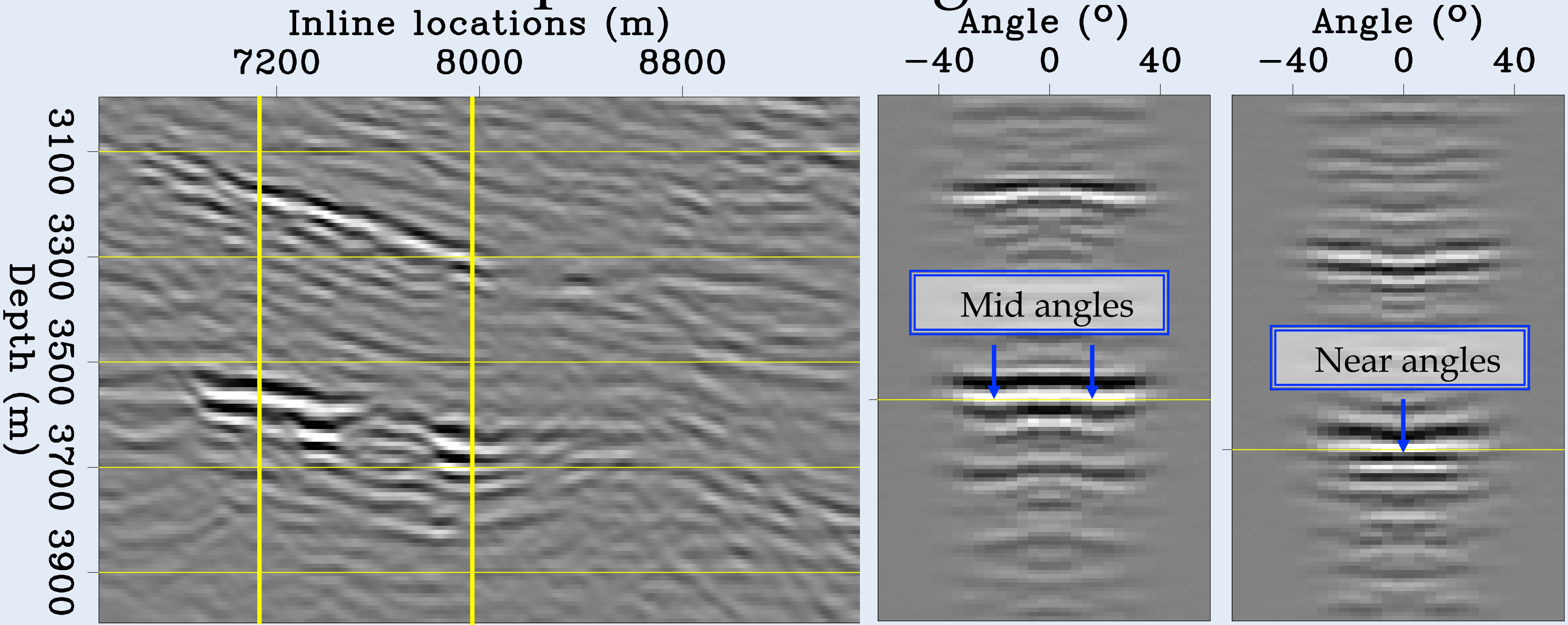

Anisotropic migration of baseline

Angle gathers of baseline

Analysis of depth-shifts in migrated images prestack images

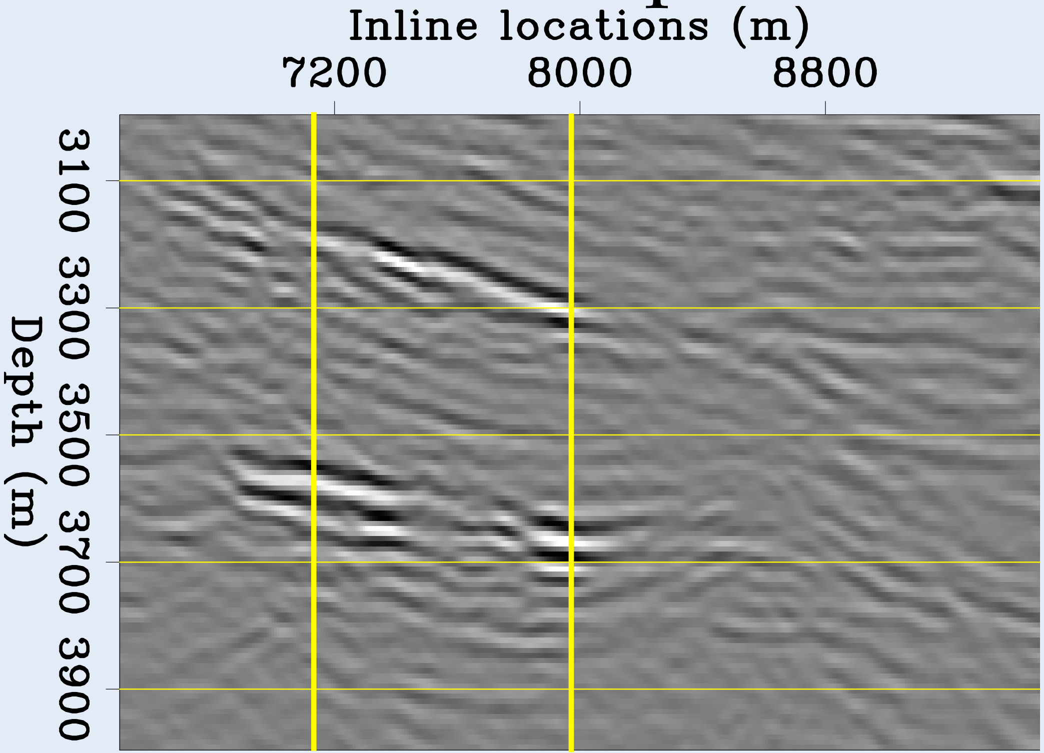

Anisotropic migration of monitor

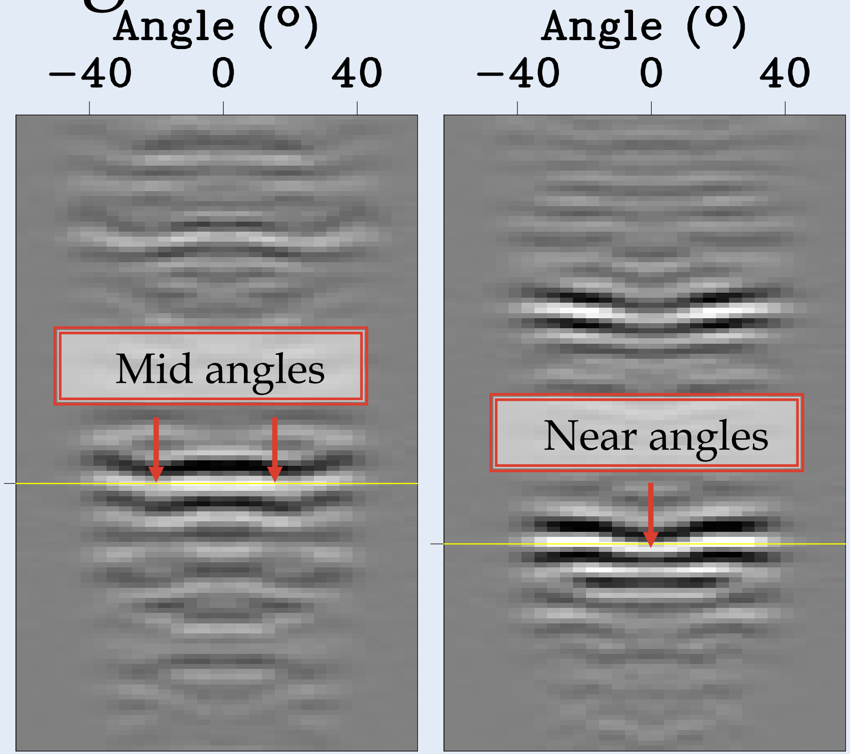

Angle gathers of monitor

- STAGE 2: *Simultaneous FWI* of baseline and monitor with the L_1 difference regularization:

$$\text{Baseline Misfit} + \text{Monitor Misfit} + \tag{4}$$

$$\beta \| |\mathbf{W}_m [\mathbf{m}_m - \mathbf{m}_b]| \|_1 . \tag{5}$$

- The L_1 norm (5) provides a **sparsifying** regularization that promotes model sparsity while still reducing spurious oscillations.

Improving resolution: the role of sparsity

- 4D phase-only FWI is to a first order $\approx$ tomographic 4D inversion (Maharramov and Biondi, 2016):

$$\begin{aligned} \|\mathbf{A}\delta\mathbf{s} - \delta\boldsymbol{\tau}\|_2 &< \sigma, \\ \|\delta\mathbf{s}\|_0 &= k, \end{aligned} \qquad (6)$$

where $\delta\boldsymbol{\tau} =$ observed time shifts, $\delta\mathbf{s}$ is the unknown slowness change, $\mathbf{A}$ is the travel-time modeling operator, σ is the 2-norm of measurement errors.

- Any minimizer $\delta\mathbf{s}$ of (6) satisfies the estimate:

$$\|\delta\mathbf{s} - \delta\mathbf{s}_0\|_2 \le \frac{2}{c_{2k}}\sigma, \qquad (7)$$

where the lower restricted isometry constant $c_{2k} = \min_{J:|J|=2k} \lambda_{\min}(\mathbf{A}_J)$.

- L_1-regularized inversion (4,5) approximates L_0 regularized inversion (Elad, 2010).
- Continuous observations boost qualitative resolution (the "peaks" of $\delta\mathbf{s}$ will stand out).

Experiment: true base

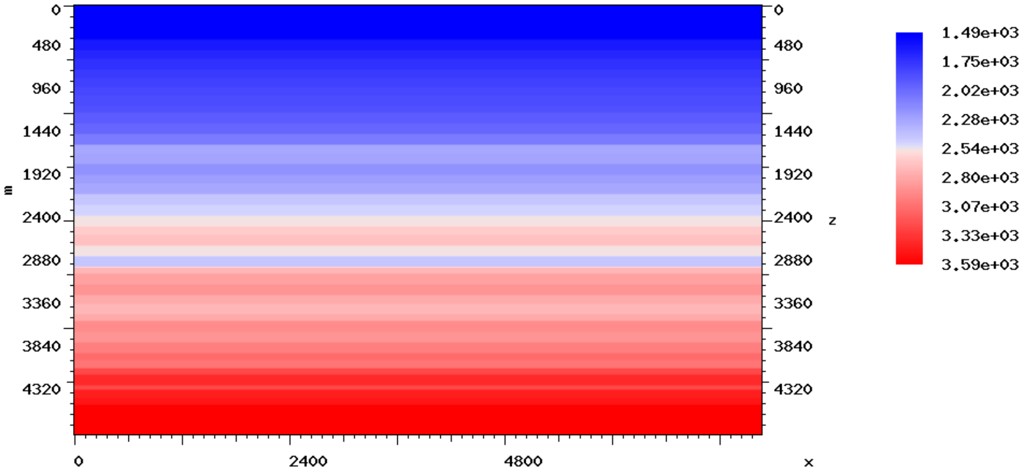

True monitor-baseline model difference at 10 m/s scale

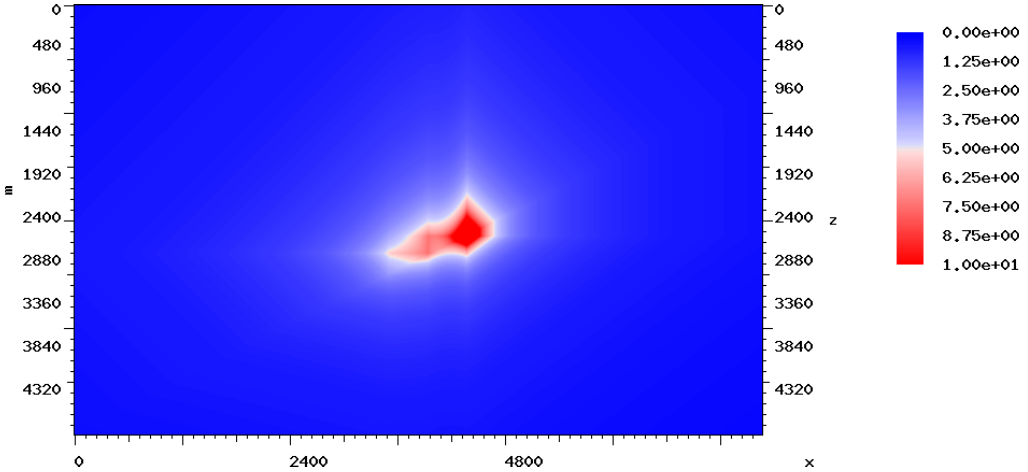

True monitor-baseline difference at 50 m/s scale

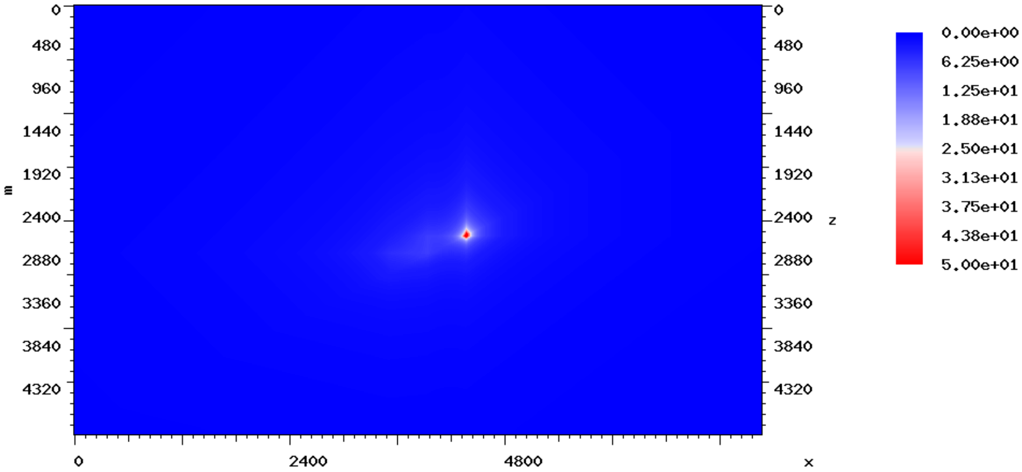

True second-first monitor model difference at 10 m/s scale

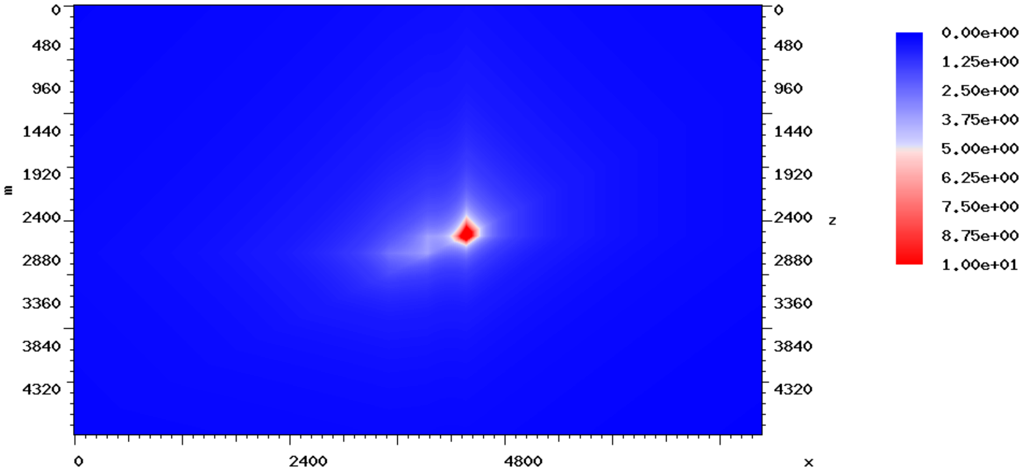

True second-first monitor model difference at 50 m/s scale

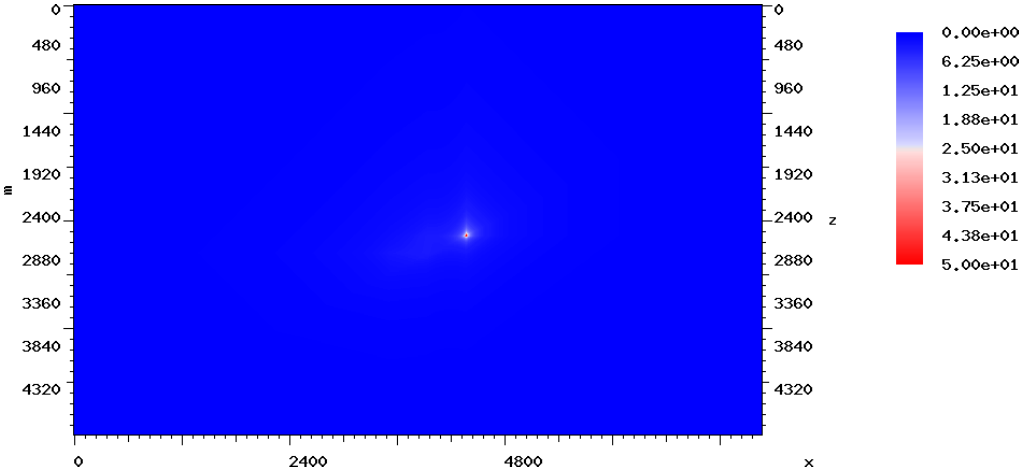

Inverted monitor-baseline difference; clean synthetics, PD FWI

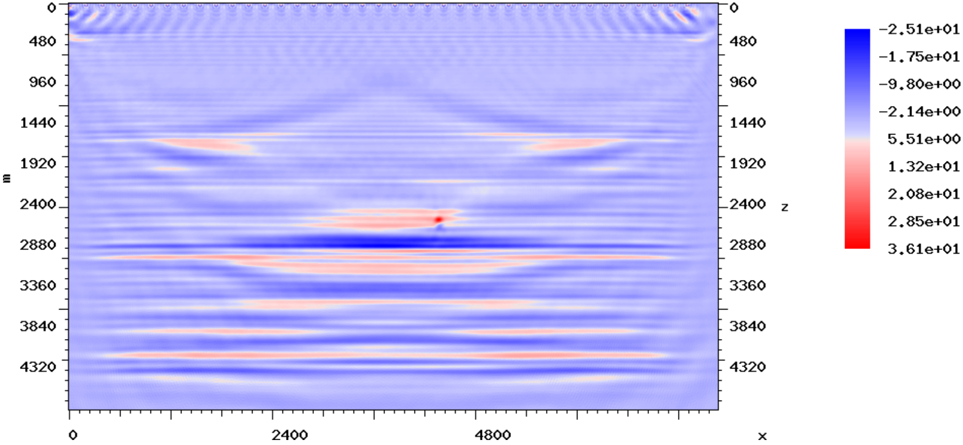

Inverted second-first monitor difference; clean synthetics, PD FWI

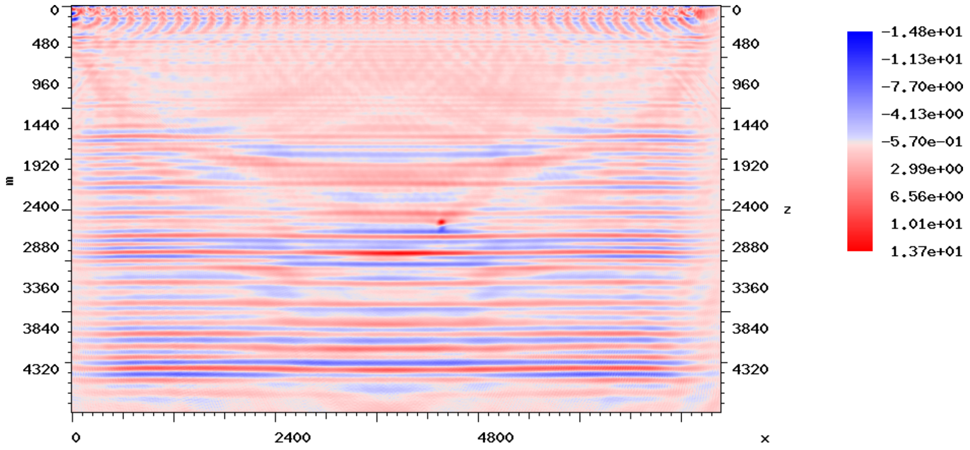

Monitor-baseline; clean synthetics, TV FWI, 10 m/s scale

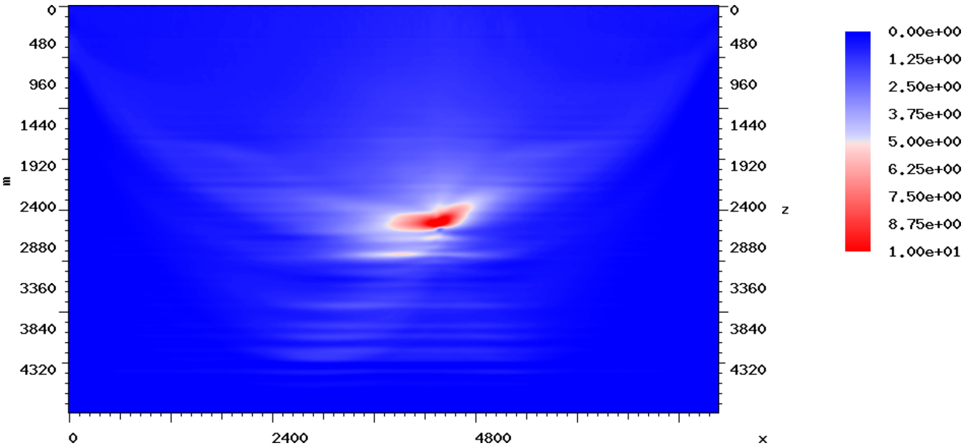

Second-first monitor; clean synthetics, TV FWI, 10 m/s scale

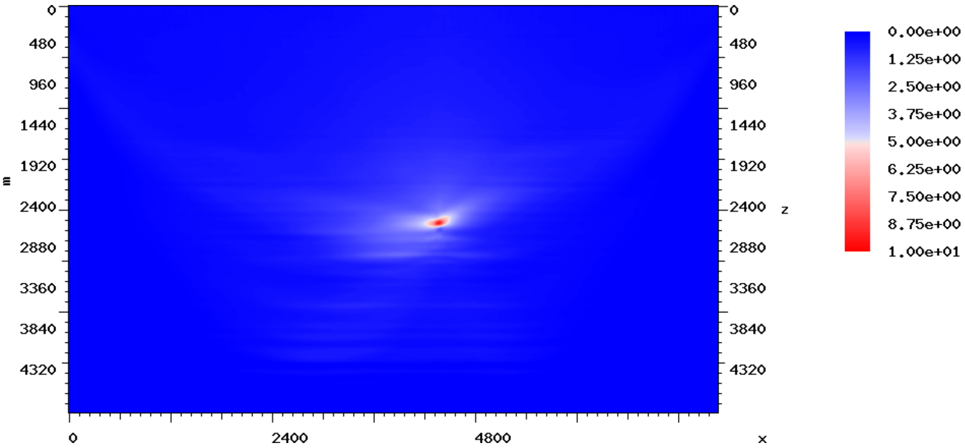

Adding white Gaussian noise

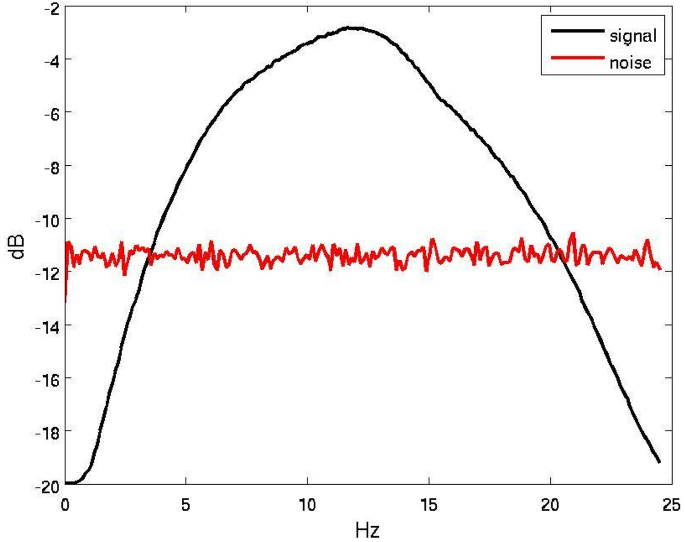

Inverted monitor-baseline difference; noisy synthetics, PD FWI

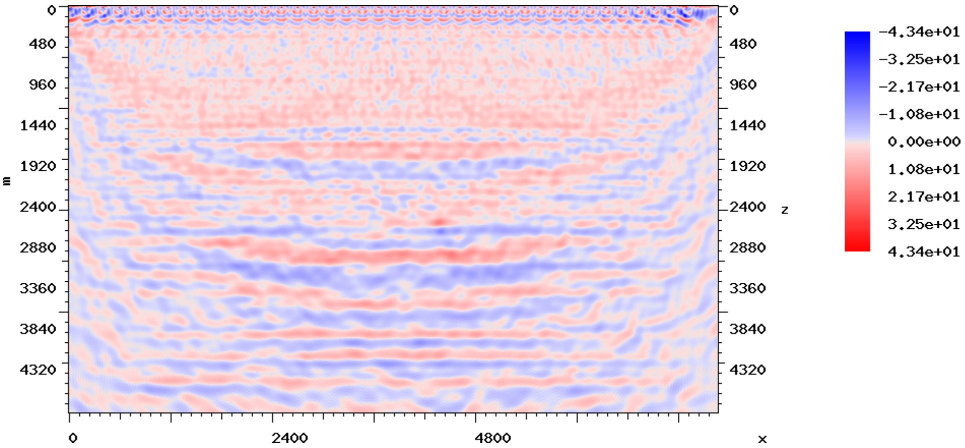

Inverted second-first monitor difference; noisy synthetics, PD FWI

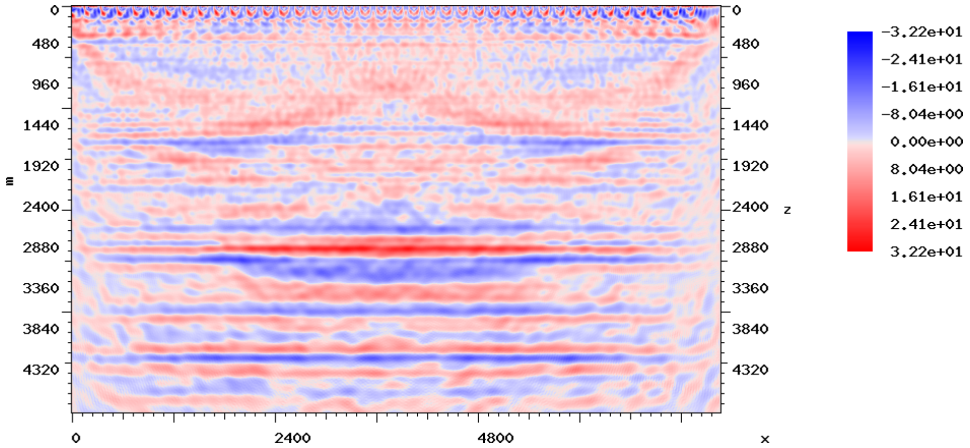

Monitor-baseline; noisy synthetics, TV FWI

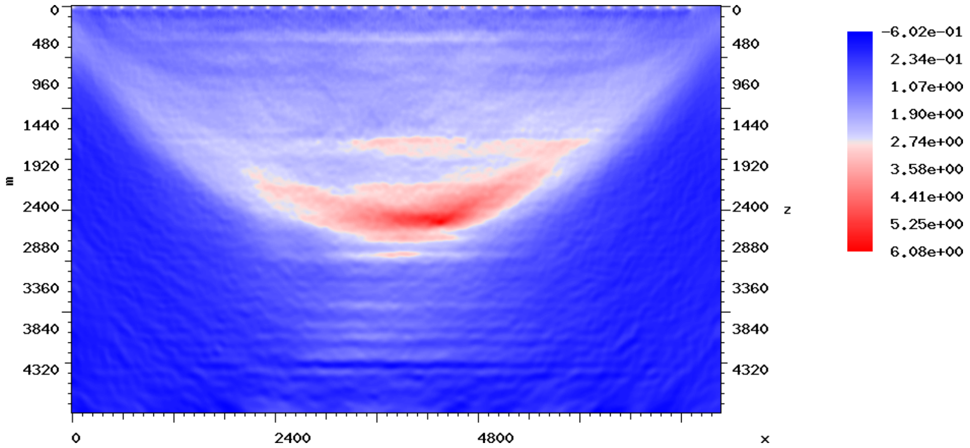

Second-first monitor; noisy synthetics, TV FWI

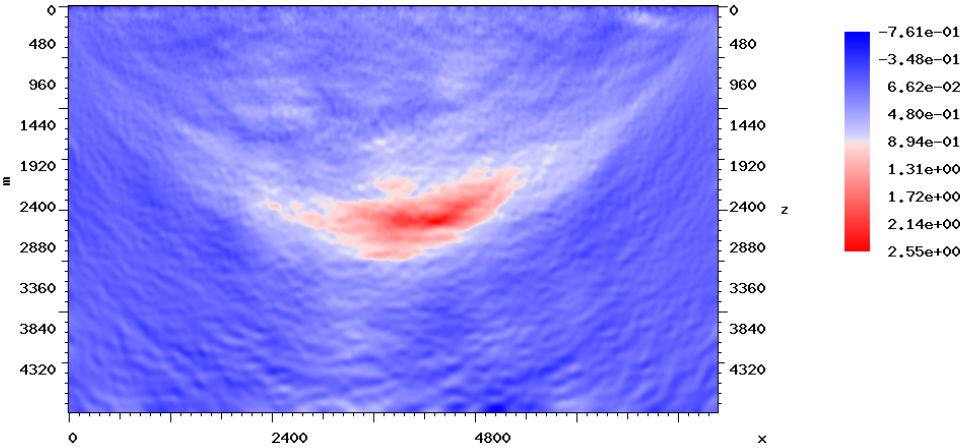

Monitor-baseline; noisy synthetics, cascaded $TV - L_1$ FWI

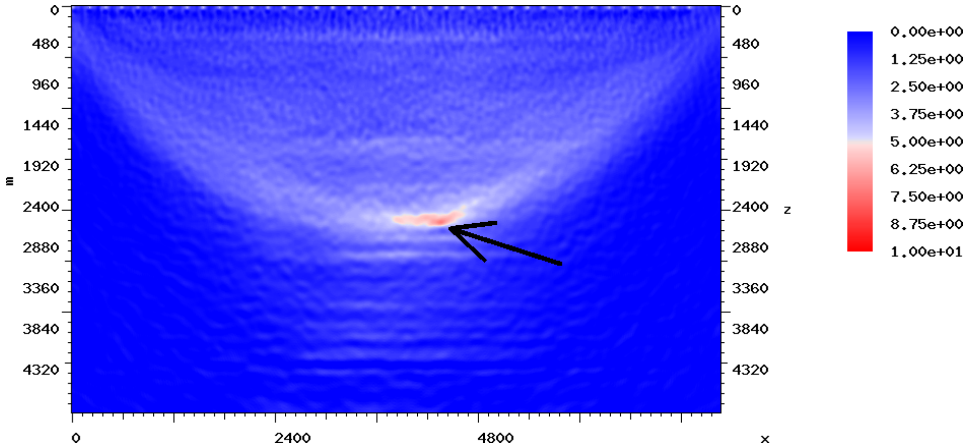

Second-first monitor; noisy synthetics, cascaded $TV - L_1$ FWI

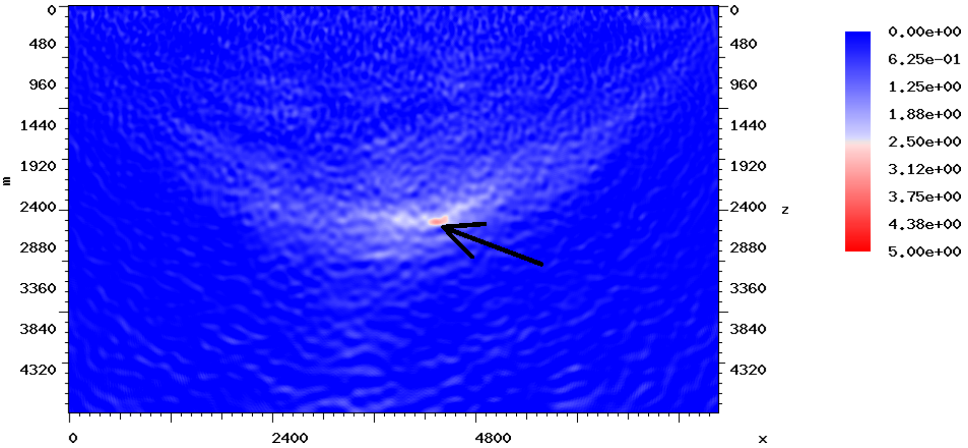

Conclusions and way forward

- Cascaded simultaneous regularized FWI **can resolve subtle subsurface velocity changes** associated with subsurface stressing in the presence of strong noise.

- Inversion can **detect relative magnitudes of velocity changes**.

- Potential applications in reservoir and earthquake monitoring, engineering geophysics.

- **Future work**: feasibility for continuous weak and passive sources.

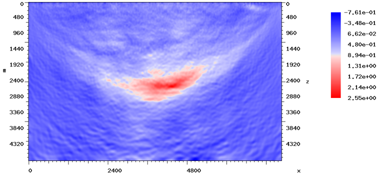
0
480
960
1440
1920
2400
2880
3360
3840
4320
m
z
0
2400
4800
x
-7.61e-01
-3.48e-01
6.62e-02
4.80e-01
8.94e-01
1.31e+00
1.72e+00
2.14e+00
2.55e+00

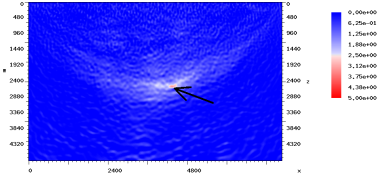
0
480
960
1440
1920
2400
2880
3360
3840
4320
m
z
0
2400
4800
x
0.00e+00
6.25e-01
1.25e+00
1.88e+00
2.50e+00
3.12e+00
3.75e+00
4.38e+00
5.00e+00

Q&A

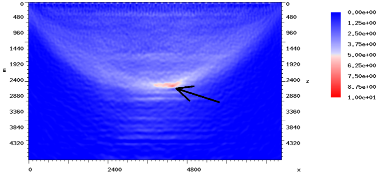
0
480
960
1440
1920
2400
2880
3360
3840
4320
m
z
0
2400
4800
x
0.00e+00
1.25e+00
2.50e+00
3.75e+00
5.00e+00
6.25e+00
7.50e+00
8.75e+00
1.00e+01